Utilizing ABAQUS' 10-Node Modified Tet for Analyzing Impact Problems Involving Thin-Walled Structures.

Ted Diehl* and Doug Carroll**
*Mechanical Technology Center, PCS
**Advanced Technology, Smart and Connected Products
Motorola
8000 W. Sunrise Blvd.
Fort Lauderdale, FL 33322
Ted.Diehl@Motorola.com

Abstract

Analyzing today's hand-held consumer electronics for impact and shock loading conditions is extremely challenging. The complex geometry and multiple contact interactions between the numerous components in a fully assembled product have made it difficult to meet development analysis schedules using traditional shell and hex element modeling approaches. The present work investigates the improvements in analysis cycle time and accuracy that can be made by utilizing the ABAQUS C3D10M tet element for these applications. Assessments of meshing speed, simplicity of contact definition, and solution accuracy and efficiency are presented.

1.0 Introduction

Performing impact analyses such as drop tests or steel ball impact tests on personal handheld electronic devices (i.e. portable phones and pagers) has proven to be a very challenging problem that requires an excessively long cycle time to complete. Many of the modelling issues stem from the complex nature of today's electronic products. The primary structural components in these devices typically consist of thin (1 mm thick) front and back thermoplastic housings, two or more printed circuit boards (PCB), connectors, sheet metal shields, elastomeric pads, batteries, metal spring contacts, and an LCD display assembly. In a typical design, the main PCB is sandwiched between the two housings with 2 to 6 screws. The other components are then stacked in the space between the main PCB and one of the housings. They are held in place with adhesives, mating features such as snaps and walls, and/or contact between the parts.

Since many of these components are thin shell-like structures, traditional modeling approaches have utilized shell-dominant meshes. Generating these meshes is by far the longest portion of the total analysis cycle time. The process of converting thousands of CAD surfaces into a shell model that accurately captures the dynamic structural behavior and assembly connectivity of the product

is a manual process that requires high levels of skill, judgement, and experience. There are many tetrahedral mesh generation tools available that can automatically generate a tet mesh from volumes of almost any complexity in just a few minutes. Provided that tets could deliver equivalent solution accuracy and reliability, a large reduction in analysis cycle time could be achieved by using auto-generated tet-dominant meshes.

Since it is likely that a handheld device may be dropped during its lifetime, it is common to analyze, with an Explicit Dynamics code, the entire structure being dropped onto a hard surface from heights ranging from 3 to 6 feet. The development of ABAQUS' new 10-node modified tet for both /Standard and /Explicit has brought with it the opportunity to utilize a significantly different and faster modeling approach for these impact analyses.

2.0   Overview of Modeling Approaches - Shells, Hexes, or Tets

There are pros and cons with each modeling approach for an impact/drop analysis. Assuming equivalent element performance, the choice boils down to a trade-off between model generation time and solver run time. Shell elements have the longest model generation times, with the smallest model sizes and fastest run times. Conversely, tet models have the shortest modeling times, largest sizes and longest run times. The best approach is the one that reduces the *total analysis cycle time*.

2.1   Shell Element Approach

A shell meshing approach ideally uses a mid-plane from the CAD geometry. For complicated geometries like a housing, it is usually not possible to obtain a mid-plane surface from the solid CAD geometry due to the many perpendicular features on the inside of a given part. As a result, the basic approach is to build a mesh of shell elements on the outside surfaces of the part geometry. Since housings are typically only one or two millimeters thick with overall lengths and widths on the order of 120 mm by 50 mm, this is often a reasonable choice. Once the outside is meshed, the inside features are meshed. Now the problem is that the mesh of the inside features and the outside surface mesh are separated by the part thickness (and may not have aligned nodes). This must be resolved either by modifying or re-building the original surface geometry or by manually extending the inside mesh to intersect with the outer mesh. Either choice is tedious and time consuming.

Another major problem with the shell modeling approach is an inability to easily transfer variations in part thickness from the CAD model directly to the associated shell elements (while ABAQUS offers a feature to do this via a table of nodal thicknesses, there is no easy way to get the data from the CAD geometry into that form). Thermoplastic parts do not have constant wall thickness. In most parts, the thickness can vary from 0.75 mm to 2 mm. The general practice is to

model the entire part with some nominal thickness or with a few different thicknesses in local regions. This approximation can cause significant errors, especially if the part is deforming in bending (for which stiffness is a function of the thickness cubed).

The inability to graphically view the element thickness makes it difficult to build the assembled model from multiple parts and also to post process it. Imagine 6 flat plates stacked one on top of the other and modeled with shell elements. Some of the shells are modeled at the mid-plane; some offset to the top, and some to the bottom (to accommodate different CAD geometry or contact constraint issues). In the pre-processor, some of these plates appear to touch one another and some have large gaps between them. There is no easy way to verify that each part's thickness is correct and that the plates are located correctly relative to each other. During the post processing from an analysis of a rigid ball being dropped on this stack of plates, there is no way to easily visualize if the displacements are correct, which plate is hitting which, or if one plate may be going through another (i.e. a contact constraint was incorrectly defined).

Additional difficulties arise from ABAQUS specific peculiarities in their contact constraints involving shell elements (similar issues occur with other FEA codes too). While two-sided contact for shells is supported in /Explicit, it is not in /Standard. Thus models used in /Standard or intended for both /Standard and /Explicit require the use of SPOS and SNEG surface definitions. With complex geometries like a housing, you will almost always get large *unwanted* overclosures because the contact surface's back side (where overclosure occurs) is infinitely deep. To avoid this, numerous smaller "patch surfaces" are required. When using double-sided contact in /Explicit, the "bullnose" assumption that is enforced in the contact logic for shells can cause numerous unwanted overclosures. In this case, the contact logic artificially extends the free edges of shell contact surfaces by 1/2 the thickness of the element. Unfortunately, you cannot easily see that this is the problem causing undesired overclosures because you get no graphical feedback showing the bullnose on the mesh [see Nagaraj (1999) for further discussion of this issue]. Debugging these types of issues is a very lengthy, manual process.

Once a shell model has been built, it does have some advantages. First, the model size is fairly small leading to fast solution times. Stress recovery with shell elements is also very good, as are displacements.

2.2   Solid Element Approach

Traditionally, Explicit codes have only supported first-order elements. Thus, to model with a solid element meant using an 8-node reduced integration hex, C3D8R. These elements are sometimes used to model parts of the product that can be meshed by an extrusion or loft of shell

elements. This limits their application to parts such as LCD's, PCB's, lenses, and pads. They cannot be used to model the complicated volumes of a housing since most meshers cannot successfully generate a hex-dominate mesh on these parts. However, when they are used, several hex elements through the thickness of the part are needed to model bending and to avoid hourglass problems. This can cause very small time steps in the /Explicit solution with thin parts. Sometimes these small elements drive the time step below 1.0E-9 seconds. At that rate, it would require over a month to solve a 5 millisecond impact event!

With the new C3D10M, a modified second-order Tet for both /Standard and /Explicit, a tetrahedral modeling approach has become a realistic option. Using a Tet modeling approach, meshes of complex housing geometry can be generated in less than an hour if the CAD database is clean and in less than a day in all but the worst case. With tets, numerous parts can be meshed relatively independently and then brought together in the final assembly with a pre-defined contact constraint definition scheme. This is difficult if not impossible to do with shells. Shell models require many interrelated modifications of each part to insure that the assembled models will match with one another in placement, thickness offset, and contact constraint definition.

Because most of the components in a portable phone are modeled using linear elastic material laws[1], many parts can be modeled with one tet element through the thickness.[2] Using a typical average element edge length of 2 mm to avoid excessively small time steps, the resulting model captures all of the local variations in part thickness with no ambiguity in the model definition. Since the entire volume is modeled, it is easy to verify part placement visually. Also, only one surface definition is generally needed for an entire part and contact constraint definitions are a simple matter of specifying that one part may contact another. Sometimes in highly curved areas of tight fitting parts, the faceted representation of the mesh can cause some overclosures between parts, but these are easily detected and resolved.

A few negative issues with the use of C3D10M meshes are large model size, longer run times, large result output databases, contact algorithm robustness, and "inaccurate" stress predictions (more to be said about this in Section 3.1). Relative to a "comparable" shell mesh, a tet mesh typically requires about 5 to 10 times more nodes and elements, runs between 5 to 15 times longer,

---

1. Despite the severe nature of dropping a portable phone/pager onto a hard floor, the event can be modelled accurately utilizing linear elastic material behavior for most of the components, including the plastic housing. In general, failure during a drop test comes from cracking or component detachment (little plasticity occurs).

2. The test cases later in the paper demonstrate that accurate solutions can be obtained with only one element through the thickness.

and generates output databases that are 5 to 10 times larger. General contact modeling using C3D10M elements in V5.8 of ABAQUS /Explicit has had several problems and bugs. Most of them generally ended with the analysis stopping due to excessive wavespeed errors. Nearly all of the known problems have been reportedly fixed in V5.8-18. These fixes are currently being tested on product-level models.

Overall, the tet element modeling approach provides a large reduction in the model generation time for hand-held electronic devices. While solution times for the tet models are much greater than the shell models, the total analysis cycle time is being reduced with the tets. As computational speeds of computer hardware continues to increase, this should only improve further.

3.0 Element Performance and Accuracy

Three test cases are utilized to assess the C3D10M's performance and accuracy. In all cases, the meshes attempt to satisfy the desire of "one element through the thickness." The first test case utilizes a cantilever beam to study in detail the element's ability to predict structural stiffness and maximum stress at the outer fiber of a structure. The second and third test cases evaluate the element's ability to predict the dynamic structural response of thin structures under shock and impact loading. For these later cases, results are compared to experimental measurements of actual structures. Where appropriate, both /Standard and /Explicit analyses are studied.

3.1 Cantilever Beam Tests

Cantilever beams geometries ranging from long slender beams (negligible shear deformation) to short stubby beams (significant shear deformation) were evaluated (Figure 1). For the three geometries tested, the long beam with a square cross-section had less than 1% shear deformation, the long rectangular beam had 4% shear deformation in the Y-direction, and the short beam with a square cross-section had approximately 20% shear deformation in both Y and Z-directions.

Also depicted in Figure 1b is the method used to enhance the estimate of outer-fiber stresses in the beam predicted by the models. Stress recovery with only one tet element (C3D10M) through the thickness can be a problem. The integration point stresses are generally good but the extrapolated nodal stresses/strains used in stress/strain contour plots can have errors in excess of 40% relative to theoretical stress predictions. For linear material models, overlaying a skin of thin membrane elements on the outside surface of the geometry can improve stress/strain recovery to within a few percent of theoretical values. This technique essentially uses the nodal motions of the tet to drive the strain and stress calculations for the membranes on the surface. Since the membranes are thin (10^{-4} times the nominal thickness of the solid geometry), their influence on the
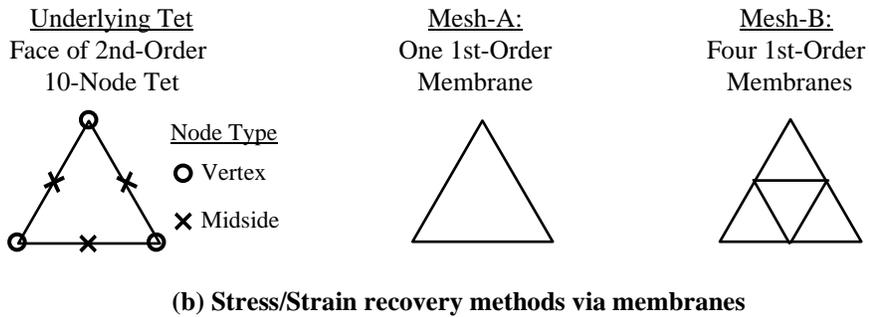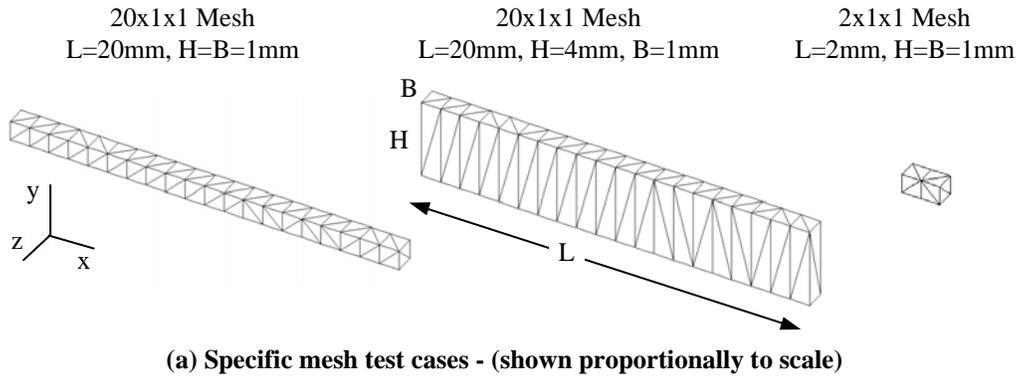
20x1x1 Mesh
L=20mm, H=B=1mm

20x1x1 Mesh
L=20mm, H=4mm, B=1mm

2x1x1 Mesh
L=2mm, H=B=1mm

(a) Specific mesh test cases - (shown proportionally to scale)

Underlying Tet
Face of 2nd-Order
10-Node Tet

Mesh-A:
One 1st-Order
Membrane

Mesh-B:
Four 1st-Order
Membranes

Node Type
O Vertex
✗ Midside

(b) Stress/Strain recovery methods via membranes

Figure 1: 10-Node tet meshes for cantilever beam tests.

component's stiffness is negligible (in fact, this stress recovery method could be done entirely as a post-processing calculation, independent of the solution). The cause of the extrapolation error in the C3D10M is currently being reviewed by HKS. Early indications are that the error is *not* necessarily a bug in the element's formulation, but rather a deficiency in the extrapolation algorithm. This may be similar to the case of the first-order reduced integration hex elements for which extrapolated nodal stresses/strains from coarse meshes are inaccurate but those recovered with a skin of membranes are much improved.

Since the C3D10M is a second-order element, the ideal choice for a "skinning element" would be a second-order membrane. Unfortunately, there are currently only first-order membranes (M3D3) in /Explicit and thus we restrict the study to their use. Provided that the nodal displacements of the tets are accurate and there are not large strain gradients from one node to the

next, then utilizing first-order membranes to skin the model is a reasonable approach. (Note that the limitation of small strain gradients between nodes can be removed if a second-order membrane is used for the skinning). Figure 1b shows two different methods to skin the second-order tet. The "Mesh-A" approach lays a single M3D3 over the entire face of the C3D10M, connecting it only to the vertices of the tet's face. The "Mesh-B" approach uses four M3D3 elements to cover a single C3D10M element face, utilizing both vertex and midside nodes from the tet.

All analysis was based on small strain, small displacement, linear elastic Timoshenko beam theory (bending plus shear deformation). Loading cases were an axial pressure applied to the right end (Px), a transverse load applied at the right end (Fy and Fz), and a uniform transverse pressure applied along the length of the beam (Py and Pz). In all cases, the beam was cantilevered from the left end. When doing such comparisons of a solid FEA model to theoretical beam analysis, it is important to apply boundary conditions that are consistent with the assumptions inherent in beam theory. This is especially important when evaluating stresses at a clamped end or when evaluating a geometry that has significant shear deformation. To ensure an appropriate comparison, the clamped boundary condition on the left end was modelled using a combination of kinematic nodal displacements on a few nodes (just enough to remove rigid body motion) and imposed nodal forces on the remainder (based on a weighting scheme described shortly). If all the nodal displacements at the cantilevered end were simply constrained in DOF 1-3, then stresses at the clamp would be distorted due to a Poisson effect. For cases of transverse loading applied to the right end, the load was distributed across the X-face of the elements to more accurately mimic the assumptions of beam theory. Since ABAQUS only supports normal pressures with *CLOAD, these loads were applied using *DLOAD. The appropriate nodal weighting was computed in a separate analysis where a normal unit pressure was applied to the elements while their nodes were completely constrained. The resulting reaction forces yielded the nodal weighting factors. It is important to note that the nodal weighting for a C3D10 is significantly different than a C3D10M.

Table 1 summarizes the results for the various beam model tests (linear Perturbation analysis in /Standard). In all cases, a Poisson's ratio of 0.3 was used (the actual values of modulus and load are not important since the results are reported normalized to the theoretical answers). The reported results are for the dominant displacement at the right end of the beam (X-disp for Px load, Y-disp for Fy load, etc.) and for the maximum stress in the X-direction on the outer fiber of the beam (located at the clamp in all cases). The results demonstrate several things. The traditional C3D10 element performs well in all cases, even the extremely tough test of the short square beam. For the case of the long rectangular beam, all the analyses (for both element types) issued warnings that every tet element was excessively distorted. Despite this warning, the C3D10 still performed superbly. The new C3D10M also performed well for predictions of displacement (which also

Table 1: Cantilever beam results for ABAQUS /Standard

• All results are normalized to the theoretical answer (i.e. FEA / Theory).

		Loading Method				
		Px	**Fy**	**Fz**	**Py**	**Pz**
Element Type	**Result type**	**Long Beam with Square Cross-Section** **20x1x1 Mesh, L=20mm, H=1mm, B=1mm.**				
C3D10 (alone)	Disp	1.00	1.00	1.00	1.00	1.00
	Stress	1.00	1.00	1.00	0.99	0.99
C3D10M (alone)	Disp	1.00	1.04	1.03	1.04	1.04
	Stress	1.00	1.38	1.40	1.34	1.38
C3D10M (M3D3, Mesh-A)	Disp	1.00	1.04	1.03	1.04	1.04
	Stress	1.00	1.04	1.04	1.01	1.01
C3D10M (M3D3, Mesh-B)	Disp	1.00	1.04	1.04	1.04	1.04
	Stress	1.00	1.06	1.05	1.04	1.04
Element Type	**Result type**	**Long Tall Beam with Rectangular Cross-Section** **20x1x1 Mesh, L=20mm, H=4mm, B=1mm.**				
C3D10 (alone)	Disp	1.00	0.99	1.00	0.99	1.00
	Stress	1.00	1.00	1.00	1.00	1.00
C3D10M (alone)	Disp	1.00	1.03	1.04	1.03	1.04
	Stress	1.00	1.39	1.41	1.36	1.39
C3D10M (M3D3, Mesh-A)	Disp	1.00	1.03	1.04	1.03	1.04
	Stress	1.00	1.03	1.04	1.00	1.02
C3D10M (M3D3, Mesh-B)	Disp	1.00	1.03	1.04	1.03	1.04
	Stress	1.00	1.06	1.07	1.06	1.05
Element Type	**Result type**	**Short Beam with Square Cross-Section** **2x1x1 Mesh, L=2mm, H=1mm, B=1mm.**				
C3D10 (alone)	Disp	1.00	0.97	0.97	0.98	0.98
	Stress	1.00	1.03	1.03	0.99	0.99
C3D10M (alone)	Disp	1.00	1.00	1.00	1.02	1.02
	Stress	1.00	1.19	1.19	1.17	1.17
C3D10M (M3D3, Mesh-A)	Disp	1.00	1.00	1.00	1.02	1.02
	Stress	1.00	0.79	0.79	0.65	0.65
C3D10M (M3D3, Mesh-B)	Disp	1.00	1.00	1.00	1.02	1.02
	Stress	1.00	0.97	0.97	0.92	0.92

indicates overall structural stiffness accuracy); all errors were less than 5%. For all the cases except axial loading, the predictions of stress using default nodal extrapolated stresses were very poor; errors ranged from 17% to 41%. However, using the skinned membrane stress recovery technique, predictions improved to less than 7% for most cases. One exception to this result was the case of using the "Mesh-A" membranes on the short square beam. For this special case, the nodal spacing is too large to expect a single first-order triangular membrane to accurately sense the stress in a structure with an axial variation in stress. The Mesh-B method yielded much improved results for that case because using the midside node had the effect of shortening the nodal spacing used in the calculation. A few cases using /Explicit were also tested for the long square beam. The loading was imposed slowly to ensure a static-like result. For the transverse loading Fy at the end of the beam, the normalized displacement result was 1.02, the normalized stress using default nodal extrapolation without membranes was 1.34, and the normalized stress using Mesh-B membranes was 1.08. In summary, these tests clearly indicate that the C3D10M performance is acceptable, provided that skinned membranes are used to recover the stresses.

3.2   Plate Shock Test

For this test, an aluminum plate is connected via four bolts to a shock table and shocked. Figure 2 shows the /Explicit FEA models used for the evaluation as well as the acceleration pulse that was recorded at the base of the bolts during the physical experiment. The actual aluminum plate was 157 mm x 76.2 mm x 1.575 mm. Relative to the plate's center, the 9.4 mm diameter hole was located x = 50.8 mm and z = 25.4 mm. A 7.62 mm diameter bolt connected the plate to the shock table. The plate was secured to the bolts by nuts on the underside of the plate. The length of the exposed bolt was 15.1 mm. For solution efficiency, 1/4 symmetry models were utilized. In the FEA models, the top of the bolt was connected to the nodes around the plate's hole with *RIGID BODY. The bottom of the bolt was constrained from motion in DOF 1, 3, 4, 5, and 6. The experimentally measured acceleration was imposed as an acceleration boundary condition in the Y-direction (using a tabular input) on the bottom node of the beam element representing the bolt.

Figure 3 depicts the results for the three FEA models tested. Both strain and absolute acceleration results are compared with experimental measurements. The data was processed consistent with the methods described by Diehl (1999). All results were appropriately sampled (anti-alias filtering employed) at 200 kHz. The results clearly show that both the S4R and the C3D10M results correlate well with the experimental measurement. The result for the C3D8R (three elements in the thickness) were quite poor. The solution showed an extreme amount of effective damping. Utilizing more elements through the thickness did not help the problem. In all the FEA models, no additional damping was used (only default Bulk Viscosity damping was
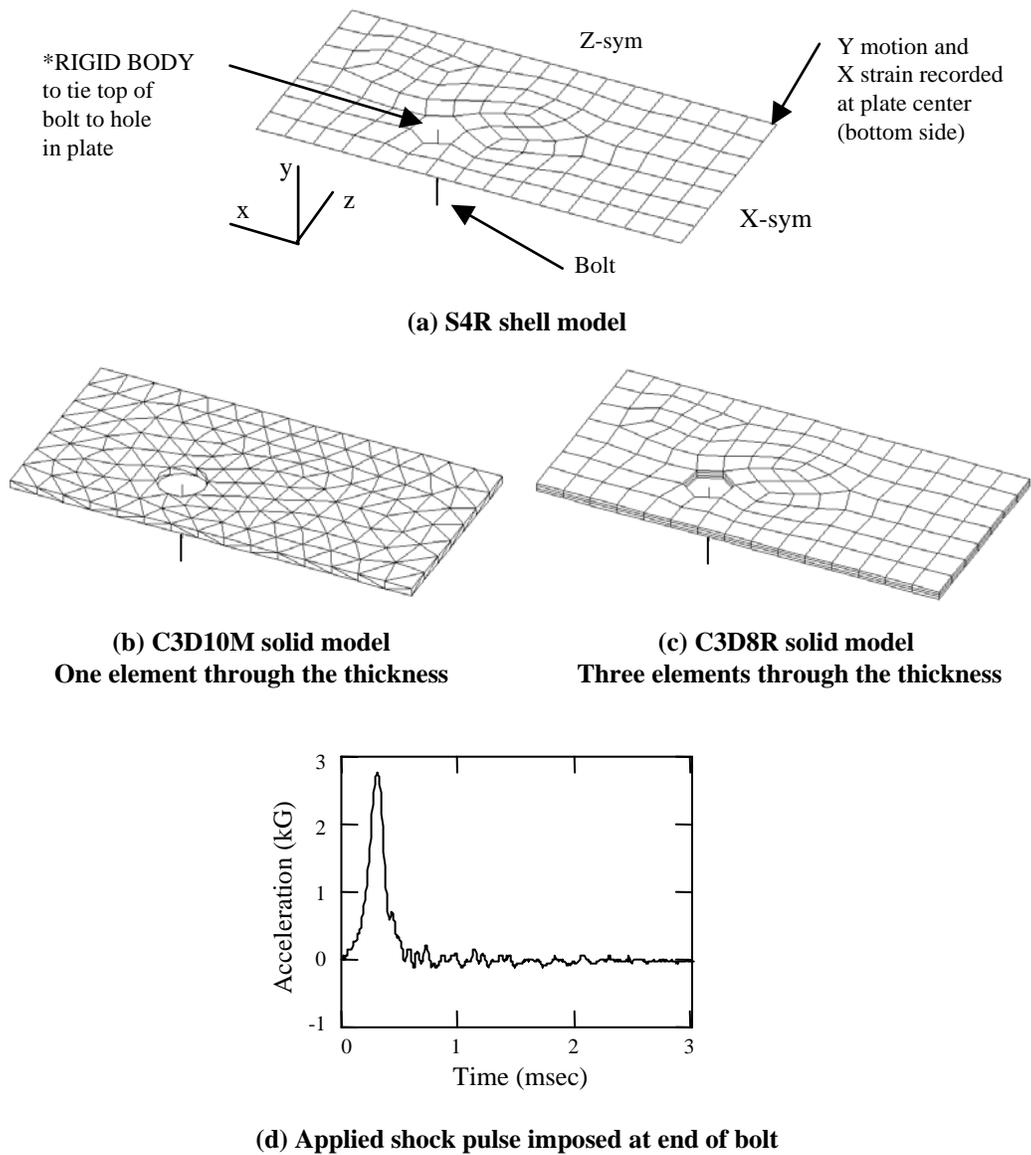
(a) S4R shell model

(b) C3D10M solid model
One element through the thickness

(c) C3D8R solid model
Three elements through the thickness

(d) Applied shock pulse imposed at end of bolt

Figure 2:   FEA models for plate shock test case
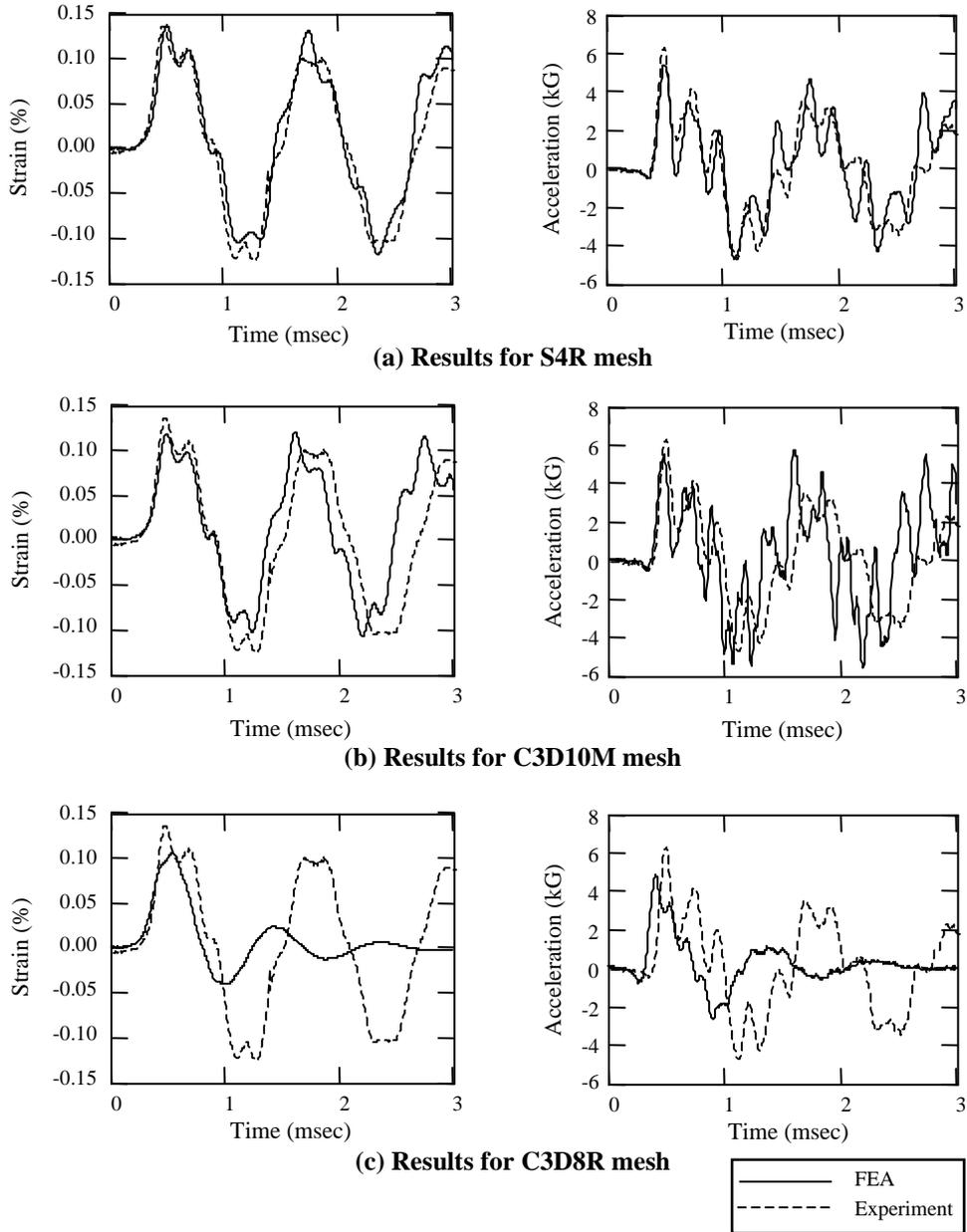
Figure 3:   Plate shock results. Strain and acceleration at center of plate.

chosen and no material damping was defined). The excessive damping in the C3D8R model is caused by the hourglass control algorithm utilized in /Explicit. For this model, the aspect ratio of the solid hexes is nearly 10:1 and this causes problems for the hourglass control scheme. It is interesting to note that as time continues, especially after 3.0 msec (not shown), the experimental results do show significant frequency-dependent material damping of the higher modes. Attempting to capture this with material damping in /Explicit is very difficult because it requires the use of stiffness proportional damping which will negatively impact the solution time increment. In summary, this test case again demonstrates that using C3D10M models with one element through the thickness yields acceptable results.

3.3   Ball Impact Test

The ball impact problem pictured in Figure 4. evaluates the accuracy of predicting the displacement at the center of an acrylic lens impacted by a 0.13 kg steel ball dropped from 500 mm. The lens is mounted in a portable-phone front housing made of polycarbonate. Further details of this test and the data processing are described by Diehl (1999). Three FEA models are used to evaluate the test. The two shell-dominant meshes use C3D8R elements to model the varying thickness lens (three C3D8R elements through the thickness). The variations in thickness for the housing itself are approximately captured by using a few shell section cards with different thicknesses. The tet model uses tets for the entire model. Both the housing and the lens are modelled with one tet through the thickness. As a point of reference, the deflection of the housing itself contributes to over 50% of the total deflection that is measured at the lens center.

Two methods of determining the maximum lens deflection were studied: 1) imposing a static indentation with the steel ball until the internal strain energy of the structure equals the initial kinetic energy of the ball just prior to impact (0.637 N·m) and 2) actually impacting the structure dynamically with the steel ball being dropped from 500 mm. Figure 5a provides the results from the first method. The results from the three FEA models showed that the S3R model was the most stiff and the C3D10M was the most flexible. The experimental result was obtained by loading the structure with an Instron. The stored strain energy was computed by integrating the experimentally recorded load-displacement curve. The load was imposed slowly to avoid any dynamic effects. Unfortunately, the lens in the prototype part cracked during this experiment at an energy of only 0.264 N·m (resulting in a displacement of 2.46 mm). To estimate what the experimental displacement would have been if the lens did not crack, this data was curve fit to a function of the square root of the energy and then extrapolated. The results shown in Figure 5a clearly show that the C3D10M model matches the static experiment the best. This is likely do to the fact that the C3D10M was able to capture the variations in housing thickness the best.
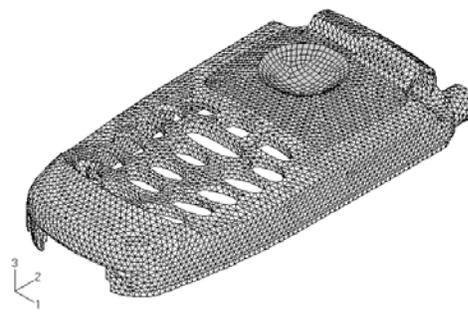
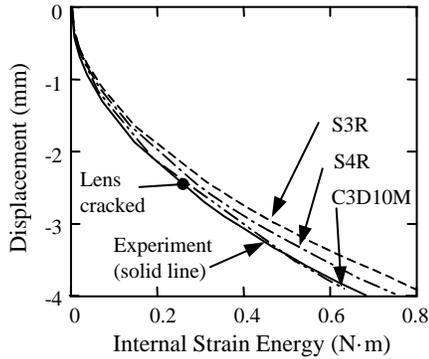**(a) Experimental set-up.**
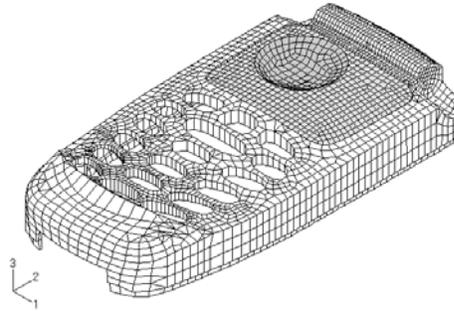
(b) S4R housing mesh (w/ C3D8R lens mesh).
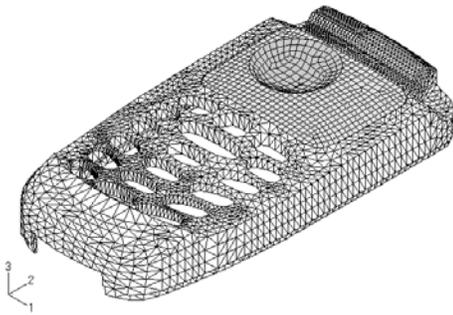
(b) S3R housing mesh (w/ C3D8R lens mesh).

**(d) All tet mesh using C3D10M.**

Figure 4: Steel ball impact example, experimental set-up and /Explicit FEA models.

Figure 5b presents the results from the dynamic tests. Two interesting things are found in these results. First, the FEA models predictions from the actual dynamic impact simulation only differed from their static energy method estimates by less than 3%, with the two shell-hex models behaving slightly softer dynamically and the tet behaving slightly stiffer dynamically. The experimental data (which was very accurately measured with a laser vibrometer that incorporated a displacement encoder) behaved 14% stiffer than the estimate from the static Instron test. Moreover, the lens did not crack. These differences in the experimental data can be explained by the fact that the plastics

Note: The static experimental measurement at left actually stopped when lens cracked at 2.46 mm. The solid line shown is an extrapolation from that point based on a curve-fit to the data before the crack. The curve-fit was a square root function of the internal strain energy.

(a) Estimates of dynamic deflection based on statics and energy methods.
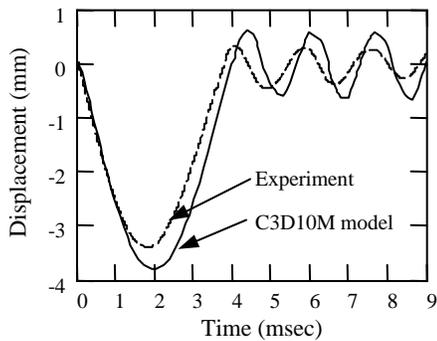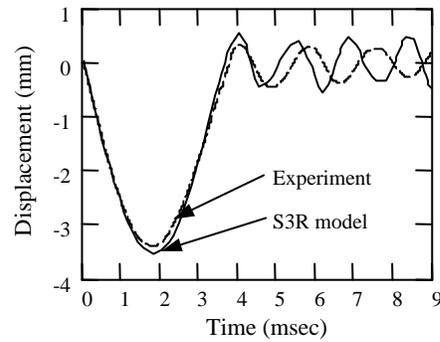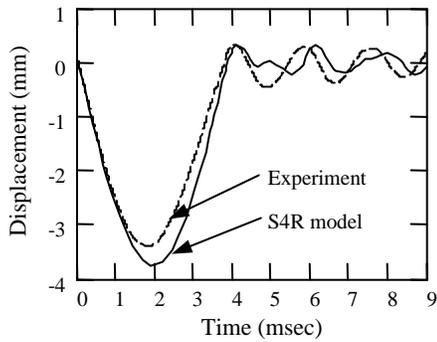
Summary

Model	Estimate via Statics + Energy Meth.	Actual Impact Result
S4R	3.68	3.76
S3R	3.49	3.53
C3D10M	3.91	3.8
Experiment	3.87	**3.39**

(b) Actual dynamic displacements: Experiment and /Explicit models.

Figure 5:   Displacement Results. Estimates of maximum deflection due to ball impact using energy methods and actual dynamic results.

used in the test are viscoelastic-viscoplastic materials. At high strain rates, the failure strain and stress increase significantly (that's why the lens did not crack during impact but did crack under static loading). Also, the modulus can increase too (this second point is generally not reported in the literature because high strain rate testing usually evaluates large strains and a 14% change in modulus is difficult to detect with the common methods used). In summary, this test again demonstrates that the C3D10M produces acceptable results. This test also indicates that a S3R-dominant mesh yields acceptable results (negligible shear locking was observed).

4.0 Conclusions

Overall, the C3D10M element modeling approach provides a reasonable alternative to the traditional shell-hex approach. Displacement predictions for the C3D10M are good, even with one element through the thickness (linear material models). Stresses predicted by default nodal extrapolation can be quite poor, but improved stresses can be obtained using a skin of membrane elements. The tet approach provides a large reduction in the model generation time for hand-held electronic devices; both meshing and contact definition are much easier. While solution times for the tet models are much greater than the shell models, the total analysis cycle time can be reduced with the tets. This should only improve as computational speeds of computer hardware increases.

Other findings from the tests are that S3R-dominant meshes may provide acceptable results. When using ABAQUS /Explicit's C3D8R element for analyzing thin structures in bending, significant errors can occur if aspect ratios for the element are not near 1:1.

Acknowledgments

References

Diehl, T., *Diehl's DSP Extensions*, 1999. Available for download at
http://mathcad.adeptscience.co.uk/dsp/

Diehl, T., Carroll, D., and Nagaraj, B. K., "Using Digital Signal Processing (DSP) to Significantly Improve the Interpretation of ABAQUS/Explicit Results," *ABAQUS Users Conference Proceedings*, May 25-28, 1999.

Nagaraj, B. K., Carroll, D., Diehl, T., "Ball Drop Simulation on Two-Way Radio Lens Using ABAQUS/Explicit," *ABAQUS Users Conference Proceedings*, May 25-28, 1999.

Gere, J. M., Timoshenko, S. P., *Mechanics of Materials - 3rd Edition*, PWS-Kent Publishing, 1990.